Environmental Science & Technology

Article

Cite This: Environ. Sci. Technol. 2019, 53, 4869−4879

pubs.acs.org/est

Assessing Air−Surface Exchange and Fate of Mercury in a Subtropical Forest Using a Novel Passive Exchange-Meter Device

Hui Zhang,[†] Luca Nizzetto,[*,∥,#] Xinbin Feng,[*,†,‡,§] Katrine Borgå,[∥,⊥] Jonas Sommar,[†] Xuewu Fu,[*,†,‡] Hua Zhang,[†,‡] Gan Zhang,[▽] and Thorjørn Larssen[∥]

[†]State Key Laboratory of Environmental Geochemistry, Institute of Geochemistry, Chinese Academy of Sciences, 99 Lincheng West Road, Guiyang, 550081, China

[‡]CAS Center for Excellence in Quaternary Science and Global Change, Xi'an, 710061, China

[§]University of Chinese Academy of Sciences, Beijing, 100049, China

[∥]Norwegian Institute for Water Research, NO-0349 Oslo, Norway

[⊥]Department of Biosciences, University of Oslo, NO-0316 Oslo, Norway

[#]Research Centre for Toxic Compounds in the Environment, Masaryk University, 601 77 Brno, Czech Republic

[▽]State Key Laboratory of Organic Geochemistry, Guangzhou Institute of Geochemistry, Chinese Academy of Sciences, Guangzhou, 510640, China

Supporting Information

ABSTRACT: A novel passive exchange meter (EM) device was developed to assess air−surface exchange and leaching of Hg in a forest floor. Flux measurements were carried out in a subtropical forest ecosystem during a full year. Over 40% of the Hg fixed in fresh forest litter was remobilized in less than 60 days in warm and humid conditions as a response to rapid turnover of labile organic matter (OM). A two-block experiment including understory and clearing showed that losses of Hg covaried with seasonal conditions and was significantly affected by forest coverage. The process controlling the bulk loss of total Hg from the litter was volatilization, which typically represented 76−96% of the loss processes (F_{loss}). The F_{loss} ranges were 520−1370 and 165−942 ng m^{-2} d^{-1} in the understory and clearing, respectively. On a yearly basis, deposition of airborne Hg exceeded total losses by a factor of 2.5 in the clearing and 1.5 in the understory. The vegetation litter in this subtropical forest therefore represented a net sink of atmospheric Hg. This study provided a novel approach to Hg air−soil exchange measurements and further insights on the link between Hg remobilization and OM turnover along with its environmental drivers.

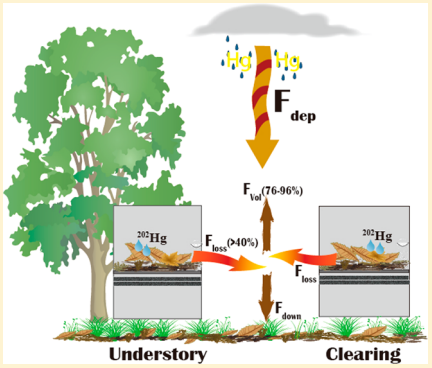

INTRODUCTION

Hg is an ubiquitous neurotoxic pollutant. Anthropogenic emissions of Hg to the atmosphere are primarily in the form of elemental mercury (Hg(0)) and divalent mercury (Hg(II)), while redox chemistry controls the transition between these two species. Hg(0) is relatively volatile, whereas Hg(II) is less volatile, more soluble, and rapidly scavenged by wet depositions and direct adsorption to soils and vegetation.[1−4] Evidences suggest that forests are important sinks of atmospheric Hg because of their scavenging, while organic soils and vegetation represent important long-term reservoirs.[5−8] Once it is introduced to the soil, Hg can undergo a methylation reaction to form a highly neurotoxic and bioaccumulative species.

Earlier assessments estimated that the global annual Hg deposition through litterfall is 1180 ± 710 Mg yr^{-1}, while OM bounded Hg in background soils and vegetation is in the order of 240000 Mg, globally.[7,9] This figure exceeds the steady state atmospheric budget of total Hg (∼5000 Mg) by 2 orders of magnitude suggesting that remobilization from aging organic matter can easily affect atmospheric loads and, consequently, global distribution. Hg emitted from soil organic matter (OM) and biomasses is calculated to represent 31% of the sum of total anthropogenic secondary emissions and natural sources.[4]

Hg(II) and Hg(0) can be adsorbed to OM through ionic exchange and simple condensation processes on organic surfaces, respectively.[10−12] These bounds are reversible, and Hg can be re-emitted if environmental conditions of OM characteristics change over time.[10,13] The predominant pool of Hg associated with OM is thought to be taken-up by the foliage and covalently fixed. To this regard, reduced sulfur groups in the OM efficiently bind Hg(II), preventing reduction processes.[9,14,15] Recent studies showed that most Hg in plant

Received: November 9, 2018
Revised: April 15, 2019
Accepted: April 16, 2019
Published: April 16, 2019

DOI: 10.1021/acs.est.8b06343
Environ. Sci. Technol. 2019, 53, 4869−4879

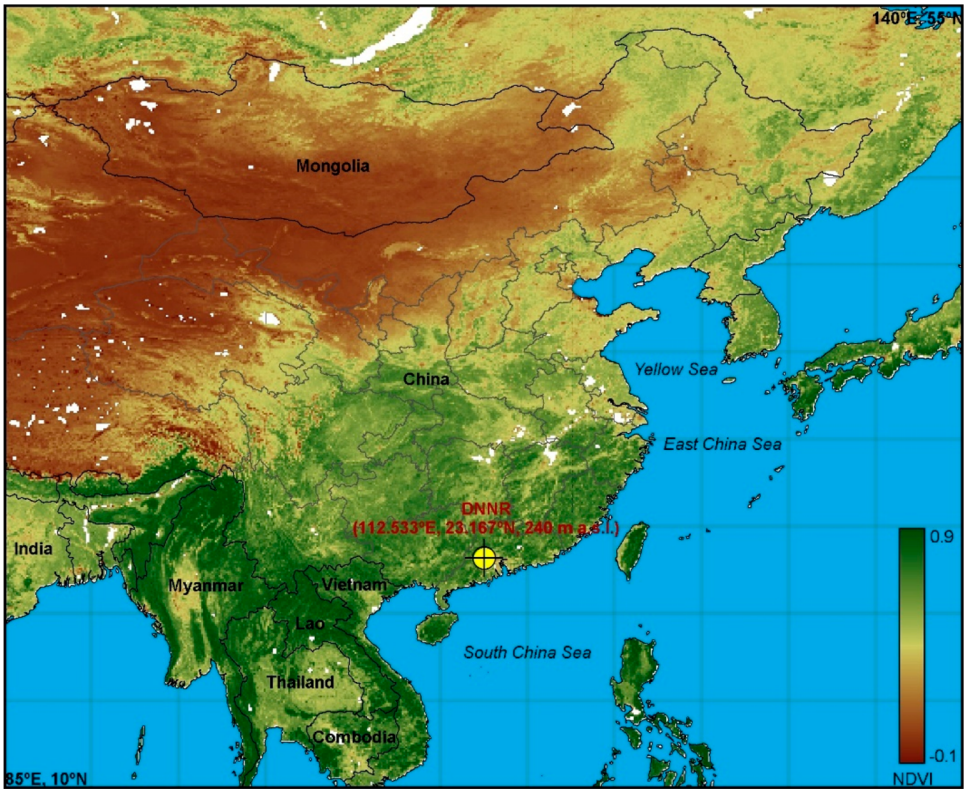

Figure 1. Location of sampling site DNNR (yellow circle) and gridded (0.1° × 0.1°) mean of monthly NDVI (satellite-based normalized difference vegetation index, representing the vegetation activity. Data were from the National Aeronautics and Space Administration Earth Observations platform) in East Asia during the study period.[8]

leaves is sequestered as divalent mercury−sulfur nanoparticles.[11] This promotes long-term storage in vegetation and soil. As expected, the re-emission of Hg to the atmosphere is therefore subordinated to the degradation of these binding structures. In nature, this can occur accidentally through fires or naturally and more diffusely through biochemical degradations.

Despite the potentially high relevance of the remobilization from vegetative soils for the global Hg mass balance, the coupling between volatilization and the turnover of labile organic matter is poorly understood. Empirical assessments are available only from few controlled laboratory experiments[16−18] which showed a correlation between Hg volatilization and OM degradation. In field assessments, correlative studies have shown a potential link between these two processes,[18,19] but a causal relationship could not be confirmed. Covariance of OM turnover with temperature and humidity can in fact blur causal relationships.

Laboratory experiments demonstrated slow mobilization of only a relatively minor fraction (between 5 and 23%) of the mass of Hg initially bound to OM in response to a 2-fold loss in the OM mass during 18 month long observations.[18] The use of traditional deposimeters to assess air−OM exchange does however not allow disentangling the influence of co-occurring processes affecting Hg and OM mass budgets. Continuous depositions of "fresh" airborne Hg during OM aging may mask volatilization fluxes.[20]

In order to study Hg mobilization from OM in forest floors at the net of atmospheric depositions in in situ OM aging experiments, we developed a novel passive exchange meter (EM) that, utilizing a mass balance approach, simultaneously and dynamically resolves OM and Hg budgets in vegetation litter over arbitrarily chosen integrated time periods. To assess causality in the relationship between litter dry mass and Hg remobilization and assess the entity of Hg fluxes under fast OM turnover, an experiment was conducted in a subtropical humid forest of southern China, subjected to monsoon climate. The subtropical monsoon climatic conditions maximize the seasonal variance of OM degradation assessed here through losses of litter dry weight and losses in organic carbon content from forest litter.

To control for possible spurious correlations between Hg remobilization and OM degradation (possibly mediated by precipitation, air humidity, or temperature as lurking variables), the experiment was conducted in two blocks using 5 replicated EMs deployed in a forest plot under a dense canopy (estimated leaf area index was 5) and 5 replicated EMs in an adjacent (less than 30 m distance) understory gap (clearing diameter was about 10 m). Previous studies showed that canopy gaps significantly inhibit degradation of litter, while experiencing nearly identical conditions of air temperature, humidity, and precipitations.[21]

MATERIAL AND METHODS

Site Description. The study site is located in the Dinghu National Nature Reserve (DNNR) area in midwestern Guangdong province, China (Figure 1). DNNR is part of the "Man and the Biosphere" (MAB) Programme of the United Nations Educational, Scientific, and Cultural Organization (UNESCO) network of protected areas. It has a typical subtropical monsoon climate with hot and wet seasons (from April to September) and dry and cold seasons (from October

DOI: 10.1021/acs.est.8b06343
Environ. Sci. Technol. 2019, 53, 4869−4879

to March) The annual average temperature is 20.9 °C with the hottest month in July (average 26.0 °C) and the coldest month in January (average 12.6 °C). The annual average rainfall is 1929 mm with 75% of precipitations occurring from March to August.[22,23] The land use is characterized by evergreen coniferous and broad-leaved mixed forests. Dominant tree species are broad-leaves (mainly *Schima superba* and *Castanopsis chinensis*) and pine needles (mainly *Pinus massoniana*). Surface litter covers 80%−90% of the ground with a thickness of 1−3 cm.[24]

Exchange Meters. The EM (Figures 2 and S1) consists of a stainless-steel tripod with a cylindrical cross-section holding

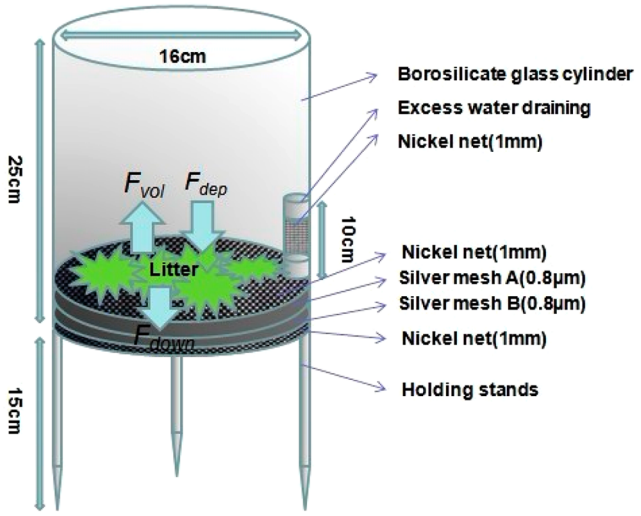

Figure 2. Diagram of the exchange meters (EMs). F_{dep} was the Hg flux deposited to the EM during the sampling period, F_{down} is the Hg flux downward export, e.g., leaching (including runoff) from EM, and F_{vol} is the Hg flux emitted up to the air from EM.

an open borosilicate glass cylinder (diameter 16 cm, height 25 cm). The glass cylinder seals two pieces of silver mesh discs (pore size of 0.8 μm, thickness 51 μm, SPI-Pore) placed at its base. Above the silver mesh, a nickel net (<2 mm mesh) is placed, holding a sample of litter collected in situ and spiked with a known amount of ^{202}Hg(II). ^{202}Hg(II) is used as a field reference to determine the volatilization and leaching fluxes (as described in a following section). This isotope is an ideal surrogate for tracking fate processes in OM as the bulk of mercury bound to forest litter is in the form of Hg(II). This is supported by previous findings showing that mercury in foliage is prevalently oxidized and exists in complex forms such as organic Hg−S species.[6,11,25−27] A small portion of Hg(II) in the litterfall may convert into Hg(0) from time to time through Hg(II) reduction, but in this form, it will be rapidly released back to the atmosphere.[28,29]

EM Handling and Sampling. For each sampling period, forest litter (including broad-leaves (mainly *Schima superba* and *Castanopsis chinensis*) and pine needles (mainly *Pinus massoniana*)) was collected from the forest site. In order to determine the water content, an aliquot of the litter was vacuum-dried for 24 h. Large dead leaves and detritus present in the remaining litter were mechanically broken down to achieve a texture with the largest pieces in the order of 1 cm^2. This was done to allow adequate homogenization and distribution of samples in replicate EMs. The remaining litter was then spiked with 2.00 μg of inorganic divalent ^{202}Hg by adding 100 mL of 20 ng/mL ^{202}Hg$(NO_3)_2$ solution to 200 g (dw) of litter. The solution of $^{202}Hg^{2+}$ was prepared by dissolving 1 mg of ^{202}HgO in 1 mL of HNO_3 solution which was diluted to 20 ng mL^{-1} by the addition of Milli-Q water. The spiked litter was transferred into an amber, borosilicate glass jar, vigorously shaken by hand for several minutes, and stored in the dark jar for at least 24 h before deployment in the field. This procedure was carried out to allow homogenization and partial redistribution of ^{202}Hg in the litter sample. The spiked litter was then distributed in situ into 10 aliquots of 20 g each and deployed in different EMs (five in understory and five in the adjacent clearing) (Figure S1). The EMs were deployed so that each spiked litter sample was only a few cm above the soil level to approximate natural exposure conditions. After field deployment, each spiked litter was sampled twice: 6 h after deployment and after two months to calculate changes in the masses of Hg (THg), ^{202}Hg, dry organic matter, organic carbon (OC), N, and water content before (t_0) and after (t_f) the exposure period. Sampling at t_0 was conducted by collecting 5 g of litter from each EM. These were carefully sealed, individually, into plastic bags and brought back to the laboratory. At t_f, the remaining litter was collected and handled in a similar way. At t_f, the silver mesh discs, conceived to sample the leaching flux of ^{202}Hg(II), were also retrieved and stored in sealed bags. Before analysis, the litter and silver meshes were stored at 4 °C. This procedure was repeated 6 times covering time intervals of two months throughout a full year.

Hg Analysis. The litter samples were freeze-dried and ground to a fine powder in a precleaned food blender (200 meshes). The blender was extensively cleaned with Milli-Q water and ethanol between different sample batches to prevent cross-contamination.[20,30] THg in litter samples was determined by a Zeeman Lumex mercury analyzer (model RA915+, Lumex Co. Inc., Russia) attached with Pyro-91 thermal decomposition accessory from Lumex Ltd. The solid samples were directly decomposed in an atomizer chamber at 800 °C with the aided catalytic action. THg was then measured by a RA-915t analyzer.[31] Standard reference samples were measured for every 10 field samples yielding recoveries in the range of 95%−105%. GBW10020 (GSB-11) was used as the litter Hg standard. Approximately, 0.15 g of each sample was digested in 50 mL of freshly mixed HNO_3/H_2SO_4 (4:1 v/v) solution for 6 h at 95 °C in a water bath.[32,33] The digested solution was then diluted by the addition of Mili-Q water to a volume of 25 mL. For Hg isotope analysis, the analyte that was preconcentrated by BrCl oxidation and $SnCl_2$ reduction was purged and trap-stepped onto a gold trap and thermo-desorbed by quadrupole inductively coupled plasma mass spectrometry (ICP-MS; Agilent 7700X). The detection limit was 100 pg/L for Hg.[34−37]

For the analysis of ^{202}Hg in the silver meshes, filters were transferred in quartz glass tubes into a furnace. The quartz tube was subsequently connected to a generator of Hg-free air (nitrogen gas, ≤0.1 ng m^{-3}). The temperature was increased to ~450 °C. The silver amalgam was then decomposed into Hg(0) vapor, which was brought by the air stream into a bubbler containing an acidic $KMnO_4$ solution that quantitatively oxidized the generated Hg(0). An aliquot of the $KMnO_4$ solution was used for analysis. Prior to analysis, excess $KMnO_4$ was reduced with $NH_2OH{\cdot}HCl$ (aq) and subsequently, Hg(II) (aq) was back-reduced to Hg(0) by the addition of $SnCl_2$ (aq). Hg(0) was subsequentely purged from the solution and

DOI: 10.1021/acs.est.8b06343
Environ. Sci. Technol. 2019, 53, 4869−4879

preconcentrated onto a gold trap to be finally quantified by ICP-MS.

QA/QC. All borosilicate glass cylinders were precleaned following the U.S. EPA Method 1631 (https://nepis.epa.gov/Exe/ZyPURL.cgi?Dockey=P1008IW8.txt). Briefly, the outside and inside surfaces of the EMs glass cylinders were first washed with laboratory analytical grade acetone in a fume hood, then washed with alkaline detergent, and finally rinsed five times with deionized water. The cylinders were immersed in 3.5% HNO_3 for 6 h at 65−75 °C through submerging the cylinders in a polyethylene bucket containing a HNO_3 solution. We ensured that all the cylinder surfaces were in contact with the HNO_3 solution. After this, the cylinders were rinsed five more times with deionized water and allowed to dry in a fume hood. They were finally placed in a muffle furnace and baked at 500 °C for 5 h. Prior to deployment, they were individually sealed in Teflon bags. In general, glass surfaces exhibit a low adsorption of mercury.[38] Nickel metal was chosen based on the same principles as the low degree of Hg amalgamation. Silver metal shows a nearly quantitative collection efficiency for Hg(0) and inorganic Hg(II) species.[39] The feasibility of using silver mesh filters as passive samplers of leaching Hg was tested prior to the experiment. The retention of Hg by the silver mesh filter was very high (95.50% and 96.84%) and was tested by feeding Hg standard solutions at different concentrations (200 and 500 pg/mL) through the silver mesh at a flow rate of 100 mL/h. In order to control for breakthrough, during field deployments, two silver meshes were piled in each EM and analyzed separately. Negligible breakthrough was observed.

Before any field deployment, the silver meshes were blanked from Hg by positioning them in a Hg free inert gas stream and heating them at 450 °C. This allowed us to reach a stable blank value of 232.7 ± 102.6 pg (n = 10). In this way, the silver mesh could be reused in subsequent deployments. After repeated uses, a visual inspection of the silver mesh occasionally revealed a patchwise change in the surface luster. This might have resulted from mechanical deterioration and/or chemical oxidation. Various treatments to restore the surface were tested. Gentle treatments with diluted acid or small amounts of commercial silver polish were generally found to produce satisfactory results.

In ICP-MS measurements, the isotopes of ^{198}Hg, ^{199}Hg, ^{200}Hg, and ^{202}Hg of the spiked sample were collected in time-resolved, single point per-peak mode with dwell times of 20 ms. Carried gas flow was optimized every day to obtain a maximum and stable signal. Detailed operating conditions for ICP-MS are listed in Table S2. A 5 mL standard solution of natural abundance (100 pg/mL) was measured prior to every 4−5 samples as a QA/QC measurement. The limit of detection for the ICP-MS measurements of ^{202}Hg isotope was 50 pg. The forest litter spiking procedure was a critical step. For the homogeneous distribution of the spiked mercury in the organic matter, we used a diluted spiking solution via diluting the concentrated ^{202}Hg solution 10 times. In this study, 17% of the mass balance assessment of Hg in the EM provided "nonsense" negative values of volatilization fluxes. This was possibly due to poor homogenization of the spiked litter. These outliers were excluded from statistical analysis.

Flux Calculations. F_{net}(ng m^{-2} d^{-1}) is the net result of all the deposition and loss processes involving THg and is calculated as

$$F_{net} = \frac{[THg_{native}{}^{litter}]_{t_f} - [THg_{native}{}^{litter}]_{t_0}}{At} = F_{dep} - F_{loss} \quad (1)$$

where $[THg_{native}{}^{litter}]_{t0}$ and $[THg_{native}{}^{litter}]_{tf}$ are initial and final amounts of total native Hg in the litter, respectively, A is the opening area of the EM (= 0.02 m^2), and $t = t_f - t_0(d)$ is the deployment time (here 60 d). F_{dep} represents the native Hg added through the various deposition processes to the EM during the sampling period while F_{loss} is the result of all the loss processes. F_{loss} can be further described as

$$F_{loss} = F_{down} + F_{vol} \quad (2)$$

where, F_{down} is the downward export flux (i.e., the leaching from the EM) and F_{vol} is the volatilization flux from the organic matter. The downward transport ($F_{down}{}^{s}$, ng m^{-2} d^{-1}) of spiked ^{202}Hg from the litter to the silver mesh disks can be measured as follows

$$F^{s}_{down} = \frac{[202_{Hg}silver]_{t_f}}{At} \quad (3)$$

where 202_{Hg}silver represents the amount of ^{202}Hg found in the silver mesh disks at the end of the exposure. From here on, the superscription "s" will indicate fluxes for ^{202}Hg. ^{202}Hg is rare in the environment; therefore, the deposition flux for this isotope is approximated to be $F_{dep}{}^{s} = 0$, and eq 1 for the labeled ^{202}Hg can be rewritten as

$$F_{net}{}^{s} = -F_{loss}{}^{s} = (F_{down}{}^{s} + F_{vol}{}^{s}) \quad (4)$$

Let us define now the function $f_{loss(t)}$ describing the instantaneous value of F_{loss}. If the concentrations of spiked ^{202}Hg in the litter are in the order of or lower than those of the native THg, and assuming the spiked ^{202}Hg behaves as its native homologue, the relationship between the instantaneous loss fluxes of native and spiked ^{202}Hg can be written as

$$f_{loss_{(t)}} = f_{loss_{(t)}}{}^{s} \quad (5)$$

where $r_{(t)} = [THg_{native}{}^{litter}]_t/[202_{Hg}litter]_t$ is the ratio between the amounts of native and spiked ^{202}Hg in the EM litter, and $f_{loss_{(t)}}{}^{s}$ is the instantaneous value of $F_{loss}{}^{s}$. Since $r_{(t)}$ is not constant (losses of native Hg are assumed to be the same as those of ^{202}Hg,; native Hg continuously receive inputs from the atmosphere), the shapes of the functions $r_{(t)}$ and $f_{loss_{(t)}}{}^{s}$ are not known. It is therefore not possible to exactly derive the value of F_{loss} for native Hg over the integrative sampling period. However, it can be argued that $r_{(t)}$ is a growing function of time, where the minimum ($r_{(t_0)}$) and maximum ($r_{(t_f)}$) values are experimentally known. Therefore, assuming in first approximation that $r_{(t)}$ is linearly growing during the two month sampling period, the following relationship can be introduced as a first approximation

$$\int_{t_0}^{t_f} r_{(t)}dt \approx \frac{(r_{(t_f)} + r_{(t_0)})}{2} = \theta \quad (6)$$

and

$$F_{loss} = \theta F_{loss}{}^{s} \quad (7)$$

Similarly, the downward export flux and volatilization flux of native Hg from the organic matter can be expressed as

$$F_{down} = \theta F_{down}{}^{s} \quad (8)$$

DOI: 10.1021/acs.est.8b06343
Environ. Sci. Technol. 2019, 53, 4869−4879

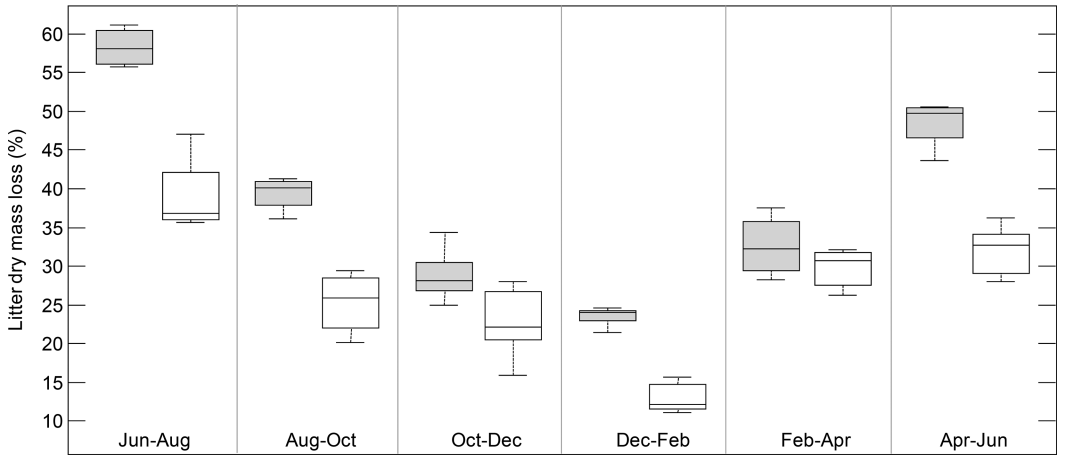

Figure 3. Bow plots of the litter dry mass loss expressed as percentage of the initial dry mass for the understory (gray boxes) and the clearing. Boxes show sample mean, 25th, and 75th percentiles. Whiskers extend to the lowest (or highest) value within 1.5 of the lower (or higher, respectively) interquartile range.

$$F_{vol} = \theta F_{vol}^{s} \quad (9)$$

Finally, from equations 1, 4, and 7, F_{dep} for native Hg can be calculated as follows

$$F_{dep} = F_{net} - \theta F_{net}^{s} \quad (10)$$

Quality of Hg Flux Measurements. Screening EM flux results for measurement quality included checking for consistency in the following assumptions: (1) the concentration of 202_{Hg}litter is in the order or lower than that of native Hg; (2) $r_{(t)}$ is a growing function of time, and therefore the condition assumed in eq 6 is verified; and (3) 202_{Hg}litter is a useful tracer of the behavior of THg. Assumption 1 is verified since r values representing the ratio of concentrations between THg and 202_{Hg}litter ranged between 18 and 20 at t_0 and 20 and 60 at t_f. This result also confirmed the validity of assumption 2 given that $r_{(t_f)}$ was always greater than $r_{(t_0)}$ (it has to be acknowledged, however, that the magnitude of the difference, $\Delta r = r_{(t_f)} - r_{(t_0)}$, has implications for tracking the accuracy of flux measurements as described above). If the growth trend of the function $r_{(t)}$ is highly non linear, the identity assumed in eq 6 can introduce an error. Assuming an unlikely worst case scenario with all deposition of Hg occurring only during the first day of exposure and considering the maximum observed values of Δr, it is possible to demonstrate that the resulting theoretical error in flux accuracy will not exceed 50% of the estimated mean value. Finally, assumption 3 has been adopted in other notable studies.[40,41]

It can be critically argued that the spiked ^{202}Hg could be more loosely bound to OM compared to the native Hg. A quick initial release of ^{202}Hg was indeed observed during the equilibration phase preceding the experiment, suggesting rapid volatilization of the superficially adsorbed pool. During the experiment, however, Δr values were directly correlated with the change in THg concentration in the litter at t_0 and t_f, showing that the increase in the r values is fully explained by the fresh deposition of native Hg on the litter and not by the higher mobilization of ^{202}Hg. An additional confirmation is that during the sampling periods of August−October and February−April, when very low net deposition of fresh THg occurred, no significant change in r values was observed.

Statistics. Normality in the distribution of replicated Hg flux measurement and litter dry mass loss was assessed using the Lillefors test with $N = 10$. To compare Hg fluxes between the canopy and gap conditions, we detrended the data set by dividing the individual flux measurement for their overall (understory and clearing) mean value within each period. We obtained two groups of data (understory and clearing) and we performed a F precision test to assess similarity in their variance. We applied the Student's t test to compare the mean of the groups in the case when the F-test was positive, and we used the Cochran's variant of the t test when the variance was significantly different. Regression models were based on the ordinary least-squares method. Correlation was quantified using Pearson's correlation coefficient. Significance of regression coefficients was tested by analysis of variance (ANOVA).

Organic Matter Analysis. Information on the method used to analyze organic matter characteristics including dry weight, total OC, and total N is presented in the Supporting Information (Text S1).

RESULTS AND DISCUSSION

Seasonality of Litter Turnover. Dry mass losses from vegetation litter measured using the EM confirmed that understory conditions significantly ($P < 0.05$) promoted turnover of OM, with dry mass losses up to 55% during the warmest and most humid periods (Figure 3). Dry mass loss data from the EM were validated by consistent measurements simultaneously performed using traditional litter bags in the understory. The data on litter degradation (i.e., mass loss) reveal the highly seasonal dynamic of OC respiration in this subtropical forest. The loss rate of litter mass had a maximum during the hot and wet seasons, in particular in June−August, then it consistently declined to a minimum in the dry and cold seasons, in particular January−March, to increase again with temperature and precipitation toward the last sampling campaign. During the dry and cold seasons, the litter deployed in the understory and the clearing experienced similar dry mass losses in the range of 15−25%; however, the variability over time of dry and OC mass loss under the canopy was 140% of that observed in the clearing. The litter degradation rate positively correlated ($P < 0.01$) with rainfall, air temperature, and humidity (Table S1) both in clearing and understory.

DOI: 10.1021/acs.est.8b06343
Environ. Sci. Technol. 2019, 53, 4869−4879

Litter mass loss is derived from the activity of detritivorous macro-invertebrates and microbes, and the loss rate depends on climate (in particular temperature and litter water content) and the nature of the litter.[42−45] A significant decline of the C/N ratio was observed during the hot and wet seasons, consistent with the period in which the highest water content in litter was measured (Table S3). The hypothesis addressed in this study is that OC mineralization and the decline of C/N drives and correlates to Hg losses from the forest litter. The water content of litter deployed in the hot and wet seasons was generally higher than that in the dry and cold seasons, probably due to heavy rainfall in the hot and wet seasons. Organic matter turnover was higher in the hot and wet seasons than in the dry and cold seasons ($p < 0.05$) and under the canopy compared to the clearing ($p < 0.05$).

Experimental observations were designed to represent two blocks (understory and clearing) where environmental conditions (i.e., rainfall, air temperature and humidity) were the same, but distinct dynamics of OM degradation occurred. The correlation among environmental condition data and litter dry mass, OC, and N loss (Table S1) showed that OM turnover was under similar drivers both in understory and clearing conditions. The clearing conditions, however, inhibited the rate of degradation, possibly due to altered water balance in the EM (e.g., more rapid evaporation in response to direct exposure to incident shortwave radiation in the clearing, compared to the understory conditions), as exhaustively discussed elsewhere.[42−46] Our results on litter mass dynamics are therefore fully consistent with previous observations in similar environments.[21]

Seasonality of ^{202}Hg Fluxes. The F_{vol}^{s} and F_{down}^{s} fluxes in each sampling period and under canopy conditions were higher in the hot and wet season than in the dry and cold season (Figure S2), suggesting that high precipitation, high temperature, and enhanced dynamics of organic matter turnover favored ^{202}Hg mobilization. To our knowledge, this is the first study to show a relationship between Hg mobilization from litter and OM turnover in field conditions.[47,48]

Organic matter in forest litter is largely constituted by complex polysaccharides including cellulose, more labile hemicellulose, and pectine.[49] Lignin is also an important component of litter; however, unlike cellulose and hemicellulose, only a limited classes of fungi and bacteria can completely mineralize it.[50,51] The observed dependence of ^{202}Hg mobilization on litter decomposition (and the conditions that promoted it) suggests that Hg might be prevalently bound to the labile constituents. Litter mass loss is derived from complete mineralization of the labile constituents and the production of water-soluble components which are then released by leaching to the underlying soil. The leaching of water-soluble constituents may contribute to the higher values of F_{down}^{s}. Similar to soil, litter (as an organic matrix) can effectively trap Hg depositions. Litter mineralization is however fast in subtropical wet forests and tightly controlled by temperature and humidity. Previous experiments in the laboratory showed that 5%−23% Hg could be released into the atmosphere during a one year litter decomposition process due to the rapid mineralization of litter carbon.[18] In our study, higher air temperature and litter moisture during the hot and wet season promoted faster decomposition of litter and Hg release. During the dry and cold season, instead, lower air temperature and lower litter moisture inhibited litter decomposition and Hg releases. Loss fluxes under the canopy were relatively high compared to the clearing. To this regard, it is important to recall that the water budget in the litter is strongly influenced by land cover. Canopies prevent rapid evaporation of water in the litter, maintaining better conditions for microorganism growth. Decomposition of litter has been observed to be generally faster in understories than in clearing.[52−54]

Fluxes of Native Hg in Litter. Hg fate in litter underwent a strong climate control during the different seasons (Figure 4). The net air−litter exchange F_{net} had positive values during October−February and April−August, and the deposition flux F_{dep} displayed a higher value in the same sampling period compared to other periods, indicating the prevailing deposition of atmospheric Hg and the forest litter serving as a net sink (Figure 4). In contrast, during the other sampling periods, the loss of Hg from litter was prevalent, primarily due to revolatilization of Hg. Generally, over the whole sampling period, both F_{vol} and F_{down} of native Hg were higher under the canopy than in the clearing. The process controlling the bulk loss of total Hg from the litter was volatilization typically representing 76%−96% of the total loss. After detrending to exclude the effect of seasonality, F_{loss} values measured under canopy throughout the year were generally higher than those in the clearing (Mann−Whitney test, $P < 0.05$; Figure 4). Data from the wetter and warmer part of the year were determinant for this result.

The total Hg loss from litter (F_{loss}, encompassing both volatilization and the leaching flux captured by the silver mesh) under the canopy was statistically correlated to litter dry mass loss, OC loss, N loss, rainfall, air temperature, and humidity (Figure 5, Table S1). These relationships dramatically fell when considering the clearing data set. The mean values of F_{loss} over the year ranged between 520 and 1370, and 165 and 942 ng m^{-2} d^{-1} in the understory and clearing, respectively. These fluxes resulted in a total loss ranging between 8% and 45% in a two month period of the total Hg present in the litter at the beginning of each exposure period. The EM method allowed the resolution of the net air−litter exchange into the volatilization and deposition components. On a yearly base, the deposition of airborne Hg during litter exposure exceeded the total losses by factors of 2.5 in the clearing and 1.5 in the understory. Vegetation litter represented therefore a net sink of atmospheric Hg. This is in agreement with previous results showing the mass of Hg in the litter of temperate forests increasing over time during litter decomposition.[18,55−57] In our study, however, we observed that the general trend was inverted during certain periods of the year, with volatilization being higher than deposition. The mechanism of Hg accumulation during litter decomposition is still uncertain. One hypothesis is that despite ongoing decomposition, binding sites for Hg on litter OM never become saturated. In this case, accumulation mechanisms will be similar to the adsorption of Hg by the cuticle of the leaf surface.[58] Another hypothesis is that the organic functional groups formed in the litter decomposition process can also serve as new binding sites.[59−61]

The first block of the experiment (understory) showed consistent results with previous laboratory-based studies in which Hg mobilization correlated with OM turnover[16−18] as well as other measured environmental variables (i.e., rainfall, air temperature, and humidity). The results of the second block (clearing), however, helped to disentangle the role of

DOI: 10.1021/acs.est.8b06343
Environ. Sci. Technol. 2019, 53, 4869−4879

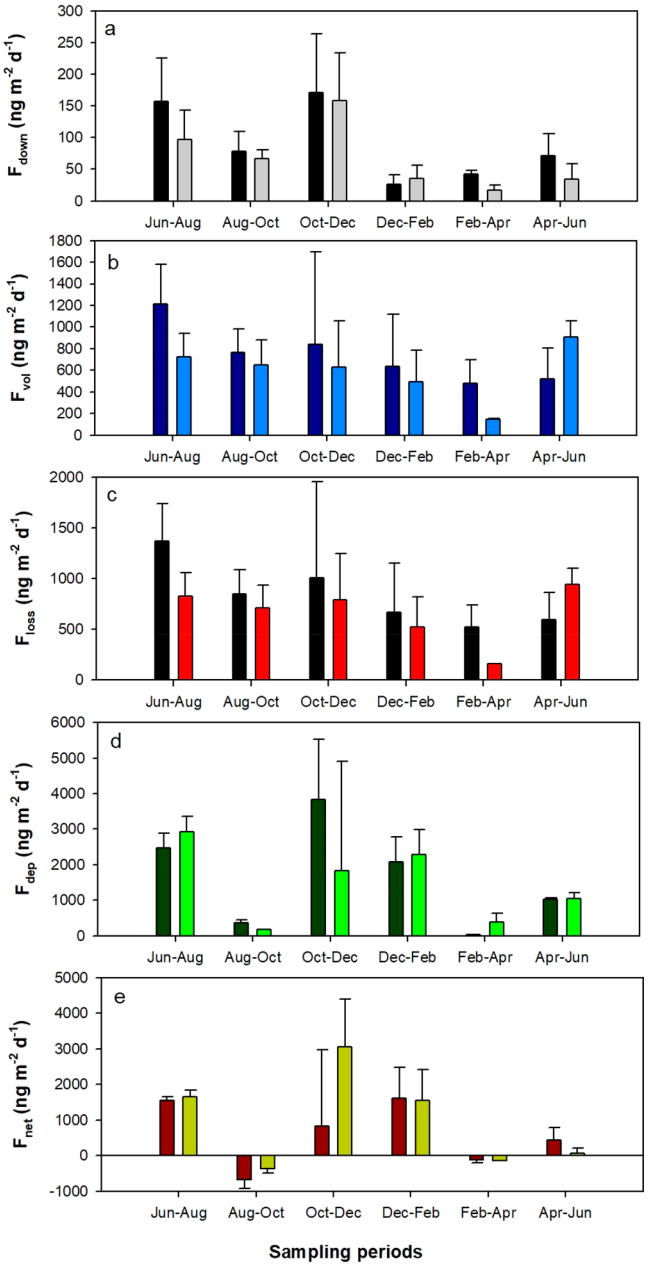

Figure 4. Hg loss, deposition, and net fluxes of native Hg as well as their volatilization and leaching components in the litter after 2 months of deployment. (a) Left (black) bars represent the leaching fluxes of native Hg (F_{down}) in the understory, and right (gray) bars represent the leaching fluxes of native Hg (F_{down}) in the clearing. (b) Left (dark blue) bars represent the volatilization fluxes of native Hg (F_{vol}) in the understory, and right (blue) bars represent the volatilization fluxes of native Hg (F_{vol}) in the clearing. (c) Left (black) bars represent the loss fluxes of native Hg (F_{loss}) in the understory, and right (red) bars represent the loss fluxes of native Hg (F_{loss}) in the clearing. (d) Left (dark green) bars represent the deposition fluxes of native Hg (F_{dep}) in the understory, and right (bright green) bars represent the deposition fluxes of native Hg (F_{dep}) in the clearing. (e) Left (dark red) bars represent the net fluxes of native Hg (F_{net}) in the understory, and right (light green) bars represent the net fluxes of native Hg (F_{net}) in the clearing.

litter degradation as a driver of Hg loss from other correlated factors (i.e., temperature and humidity). Despite the clearing and the understory set experiencing the same average

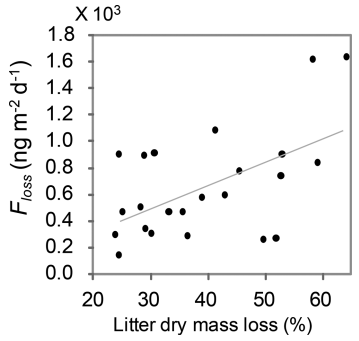

Figure 5. Scatter plot and first order least-squares model for F_{loss} vs litter dry mass loss.

conditions of temperature, waterfall, and air humidity, no significant correlation was observed in the clearing with temperature and humidity. Only a positive correlation with N loss ($P < 0.05$) was observed, corroborating the hypothesis that higher Hg mobilization fluxes under and outside canopies were primarily driven by litter OM turnover.

Lack of significant correlation between F_{loss} and litter dry mass loss observed in the clearing could have been determined by either lack of statistical resolution due to the limited variance of OM degradation rate (in comparison to the forest block) or by the influence of an emerging confounding factor associated with the clearing conditions, possibly controlling Hg dynamics (e.g., direct exposure to solar radiation during some hours of the day), alone or in combination. The comparison of the residuals from the correlation between F_{loss} values and the first order least-squares model linking F_{loss} and dry mass loss in the understory and clearing conditions helps to evaluate these cases. Consistent scedasticity (Figure S3) was observed for the residuals from the understory and clearing data sets, suggesting common drivers in the relationships linking Hg and dry mass losses. Such a consistent behavior supports the hypothesis that F_{loss} is under the same biogeochemical drivers in the understory and the clearing, while the lack of correlation with the OM loss flux in the clearing was likely due to the insufficient variability of OM degradation rates measured in the clearing during the year.

Total Hg loss rates observed in the present study were much higher (about 1 order of magnitude) than those previously observed in laboratory-based studies[16−18] or in previous field studies[19] reporting limited mobility of OM-bound Hg. Our study is the first to be performed in a subtropical warm and humid environment. OM degradation rates measured here were 1 order of magnitude higher than those reported in previous studies.[18] Additionally, the litter decomposition rate is strongly influenced by the type of litter. In general, the litter decomposition rate is higher for subtropical forests dominated by evergreen or deciduous broadleaf species than for coniferous forests with pine needles.[57,62−64] Inclusively, lower capacities to accumulate Hg in the former than the latter were also observed.[56,65] Remarkably, the only available theoretical assessment of the influence of OM turnover on the global mass balance of Hg was performed taking into consideration parameters derived for temperate and boreal environments.[9] Subtropical and tropical forests represent more than 50% of the total forest land cover. Assessments of the global mass balance of Hg could therefore have significantly underestimated the influence of the rapid turnover of Hg fixed in the litter and superficial soil of subtropical and tropical humid

DOI: 10.1021/acs.est.8b06343
Environ. Sci. Technol. 2019, 53, 4869−4879

climates. Therefore, the enhanced mobility of Hg shown here deserves further scientific attention, especially when assessing general fate and distribution of Hg under a globally warming climate.

Significance of EM Based Measurements and Comparisons with Previous Studies. The conventional and widely used technique to measure the air−surface exchange flux of Hg(0) is the DFC method.[66−68] Hg(0) emission fluxes from deciduous forest soils previously collected using this method are summarized in Table S4. The mean volatilization flux (668 ng m^{-2} d^{-1}) calculated in the present study was somehow higher, but in the same order of magnitude, than previously reported observations by DFC (Table S4) (12−498 ng m^{-2} d^{-1}) with a mean of 221 ng m^{-2} d^{-1}. Similarly, the volatilization fluxes estimated in the present study were comparable to (although slightly higher) those measured by DFC in a study in Mt. Jinyun of China in a similar forest ecosystem (342−498 ng m^{-2} d^{-1}).[69] These differences are not surprising as the DFC measurements target the volatilization flux at the net of gaseous depositions, while the flux calculated through the EM represents the total volatilization. This fully explains the offsets existing between the data sets. It must also be recalled that similar to the EM method, DFC flux measurements are also affected by uncertainties.[70−74]

Previous DFC-based measurements have shown both prevailing volatilization or depositions varying from case to case.[70,75,76] In contrast, measurements using the EM quantify the total deposition flux including contributions from gaseous oxidized mercury (GOM) and particulate bound mercury (PBM) dry and wet deposition (mostly from throughfall) besides the total gaseous depositions of Hg(0). Net deposition fluxes estimated from the EM approach (annual mean of 276 μg m^{-2} yr^{-1}) suggested that the DNNR forest was a net sink of Hg. This conclusion is also supported by earlier findings which showed that throughfall Hg fluxes (40−113 μg m^{-2} yr^{-1}) were significantly higher than the Hg(0) emission fluxes in China.[75,77−79]

Uncertainties in conventional flux measurements and emission estimates (including primary and secondary sources) hinder confidence in current global and regional Hg budgets.[4,76,80] The proposed EM methods can constrain some of these uncertainties, delivering long-term temporally integrated flux measurements. Globally, the variability of air−surface exchange flux measurements is larger for forest systems (−727 to +707 Mg yr^{-1}) than other terrestrial ecosystems.[81] When the results generated in the present study are applied to the total forested area of China (http://www.resdc.cn/data.aspx?DATAID=99), in first approximation, the net Hg deposition fluxes are calculated to be roughly 73 Mg yr^{-1} for the broadleaf forests and 240 Mg yr^{-1} for the coniferous forests. It should be emphasized that the air−surface exchange process is strongly dependent on land cover and climate.[59,82−84] For example, the THg mass positively correlated with the latitude with an average mass increase of 10.6 g ha^{-1} per degree latitude.[59,82] High contents of Hg in litterfall and throughfall were observed in coniferous forests,[56,62,85,86] confirming boreal forests as important capacitors for Hg. Therefore, we recommend the expansion of the application of EM to address the ecosystem exchange of Hg in different forest biomes.

■ ASSOCIATED CONTENT

Supporting Information

The Supporting Information is available free of charge on the ACS Publications website at DOI: 10.1021/acs.est.8b06343.

Additional information on the Pearson correlation coefficients and P values of the correlation analysis, detailed operating conditions for ICP-MS, the trends of mean air temperature, rainfall, water content and C/N in every sampling period, Hg(0) emission fluxes from deciduous forest soils collected by DFC method, the field deployment and mass balance of Hg in the exchange meters (EMs), fluxes of ^{202}Hg in the litter after 2 months of deployment and the consistent scedasticity for the residuals from the understory and clearing data sets (PDF)

■ AUTHOR INFORMATION

Corresponding Authors

*Tel: +86 851 85891356. Fax: +86 851 85891609. E-mail: fengxinbin@vip.skleg.cn.

*Tel: +86 851 85891508. Fax: +86 851 85891609. E-mail: fuxuewu@mail.gyig.ac.cn.

*Tel: +47 22 18 51 00. Fax: +47 22 18 52 00. E-mail: luca.nizzetto@niva.no.

ORCID

Xinbin Feng: 0000-0002-7462-8998

Katrine Borgå: 0000-0002-8103-3263

Xuewu Fu: 0000-0002-5174-7150

Gan Zhang: 0000-0002-9010-8140

Notes

The authors declare no competing financial interest.

■ ACKNOWLEDGMENTS

This research was financially supported by the Research Council of Norway under the programme NORKLIMA "Mechanisms of the air−surface exchange of organic pollutants and mercury in a Chinese subtropical forest (EXPOLL, 193608/S30 2010-2012)" and the National Science Foundation of China (41430754, 41703134, 41622305). We also thank Xiang Liu, Lili Ming, Liwei Cui, and Yupeng Cheng for their assistance with sampling and analysis.

■ REFERENCES

(1) Lindberg, S. E.; Stratton, W. J. Atmospheric mercury speciation: Concentrations and behavior of reactive gaseous mercury in ambient air. *Environ. Sci. Technol.* **1998**, *32* (1), 49−57.

(2) St. Louis, V. L.; Rudd, J. W. M.; Kelly, C. A.; Hall, B. D.; Rolfhus, K. R.; Scott, K. J.; Lindberg, S. E.; Dong, W. Importance of the forest canopy to fluxes of methyl mercury and total mercury to boreal ecosystems. *Environ. Sci. Technol.* **2001**, *35* (15), 3089−3098.

(3) Poissant, L.; Pilote, M.; Xu, X. H.; Zhang, H.; Beauvais, C. Atmospheric mercury speciation and deposition in the Bay St. Francois wetlands. *J. Geophys. Res.* **2004**, *109* (D11), 4364 DOI: 10.1029/2003JD004364.

(4) Pirrone, N.; Cinnirella, S.; Feng, X.; Finkelman, R. B.; Friedli, H. R.; Leaner, J.; Mason, R.; Mukherjee, A. B.; Stracher, G. B.; Streets, D. G.; Telmer, K. Global mercury emissions to the atmosphere from anthropogenic and natural sources. *Atmos. Chem. Phys.* **2010**, *10* (13), 5951−5964.

(5) Gustin, M. S.; Engle, M.; Ericksen, J.; Xin, M.; Krabbenhoft, D.; Lindberg, S.; Olund, S.; Rytuba, J. New insights into mercury exchange between air and substrate. *Environ. Sci. Technol.* **2005**, *69* (10), A700−A700.

DOI: 10.1021/acs.est.8b06343
Environ. Sci. Technol. 2019, 53, 4869−4879

(6) Laacouri, A.; Nater, E. A.; Kolka, R. K. Distribution and Uptake Dynamics of Mercury in Leaves of Common Deciduous Tree Species in Minnesota. *Environ. Sci. Technol.* **2013**, *47* (18), 10462−10470.
(7) Wang, X.; Bao, Z. D.; Lin, C. J.; Yuan, W.; Feng, X. B. Assessment of Global Mercury Deposition through Litterfall. *Environ. Sci. Technol.* **2016**, *50* (16), 8548−8557.
(8) Jiskra, M.; Sonke, J. E.; Obrist, D.; Bieser, J.; Ebinghaus, R.; Myhre, C. L.; Pfaffhuber, K. A.; Wangberg, I.; Kyllonen, K.; Worthy, D.; Martin, L. G.; Labuschagne, C.; Mkololo, T.; Ramonet, M.; Magand, O.; Dommergue, A. A vegetation control on seasonal variations in global atmospheric mercury concentrations. *Nat. Geosci.* **2018**, *11* (4), 244−250.
(9) Smith-Downey, N. V.; Sunderland, E. M.; Jacob, D. J. Anthropogenic impacts on global storage and emissions of mercury from terrestrial soils: Insights from a new global model. *J. Geophys. Res.* **2010**, *115*, 115.
(10) Farella, N.; Lucotte, M.; Davidson, R.; Daigle, S. Mercury release from deforested soils triggered by base cation enrichment. *Sci. Total Environ.* **2006**, *368* (1), 19−29.
(11) Manceau, A.; Wang, J. X.; Rovezzi, M.; Glatzel, P.; Feng, X. B. Biogenesis of Mercury-Sulfur Nanoparticles in Plant Leaves from Atmospheric Gaseous Mercury. *Environ. Sci. Technol.* **2018**, *52* (7), 3935−3948.
(12) Tsui, M. T. K.; Finlay, J. C.; Nater, E. A. Effects of Stream Water Chemistry and Tree Species on Release and Methylation of Mercury during Litter Decomposition. *Environ. Sci. Technol.* **2008**, *42* (23), 8692−8697.
(13) Zhang, H.; Lindberg, S. E. Processes influencing the emission of mercury from soils: A conceptual model. *Journal of Geophysical Research: Atmospheres* **1999**, *104* (D17), 21889−21896.
(14) Skyllberg, U.; Xia, K.; Bloom, P. R.; Nater, E. A.; Bleam, W. F. Binding of mercury(II) to reduced sulfur in soil organic matter along upland-peat soil transects. *Journal of Environmental Quality* **2000**, *29* (3), 855−865.
(15) Khwaja, A. R.; Bloom, P. R.; Brezonik, P. L. Binding constants of divalent mercury (Hg^{2+}) in soil humic acids and soil organic matter. *Environ. Sci. Technol.* **2006**, *40* (3), 844−849.
(16) Fritsche, J.; Obrist, D.; Alewell, C. Evidence of microbial control of Hg^0 emissions from uncontaminated terrestrial soils. *J. Plant Nutr. Soil Sci.* **2008**, *171* (2), 200−209.
(17) Obrist, D.; Fain, X.; Berger, C. Gaseous elemental mercury emissions and CO_2 respiration rates in terrestrial soils under controlled aerobic and anaerobic laboratory conditions. *Sci. Total Environ.* **2010**, *408* (7), 1691−1700.
(18) Pokharel, A. K.; Obrist, D. Fate of mercury in tree litter during decomposition. *Biogeosciences* **2011**, *8* (9), 2507−2521.
(19) Hintelmann, H.; Harris, R.; Heyes, A.; Hurley, J. P.; Kelly, C. A.; Krabbenhoft, D. P.; Steve Lindberg, O.; Rudd, J. W. M.; Scott, K. J.; Louis, V. L. S. Reactivity and mobility of new and old mercury deposition in a boreal forest ecosystem during the first year of the METAALICUS study. *Environ. Sci. Technol.* **2002**, *36* (23), 5034−5040.
(20) Wang, X.; Lin, C. J.; Lu, Z. Y.; Zhang, H.; Zhang, Y. P.; Feng, X. B. Enhanced accumulation and storage of mercury on subtropical evergreen forest floor: Implications on mercury budget in global forest ecosystems. *J. Geophys. Res.: Biogeosci.* **2016**, *121* (8), 2096−2109.
(21) Zhang, Q. H.; Zak, J. C. Effects of Gap Size on Litter Decomposition and Microbial Activity in a Subtropical Forest. *Ecology* **1995**, *76* (7), 2196−2204.
(22) Zhang, N.; Qiao, Y. N.; Liu, X. Z.; Chu, G. W.; Zhang, D. Q.; Yan, J. H. Nutrient Characteristics in Incident Rai nfall, Throughfall, and stemflow in Monsoon Evergreen Broad -leaved Forest at Dinghushan. *Journal of Tropical and Subtropical Botany* **2010**, *18* (5), 502−510.
(23) Long, X. J.; Wang, X. M.; Zhu, S. J.; Wang, Y. S.; Dong, H. Y.; Huang, Z. L.; Chen, Y. J.; Bao, R. Y.; Wu, Z.Y. Variation and source analysis of atmospheric organic acids fromprecipitation at Dinghu Mountain. *Environmental Chemistry* **2011**, *30* (9), 1612−1619.
(24) Chunlin, C. L.; Zhou, G. Y.; Wang, X.; Tang, X. L.; Zhou, C. Y.; Yu, G. R. Below-canopy CO_2 flux and its environmental response characteristics in a coniferous and broad-leaved mixed forest in Dinghushan, China. *Acta Ecologica Sinica* **2007**, *27* (3), 846−854.
(25) Lindberg, S. E.; Meyers, T. P.; Taylor, G. E.; Turner, R. R.; Schroeder, W. H. Atmosphere-Surface Exchange of Mercury in a Forest - Results of Modeling and Gradient Approaches. *J. Geophys. Res.* **1992**, *97* (D2), 2519−2528.
(26) Frescholtz, T. F.; Gustin, M. S.; Schorran, D. E.; Fernandez, G. C. J. Assessing the source of mercury in foliar tissue of quaking aspen. *Environ. Toxicol. Chem.* **2003**, *22* (9), 2114−2119.
(27) Sheehan, K. D.; Fernandez, I. J.; Kahl, J. S.; Amirbahman, A. Litterfall mercury in two forested watersheds at Acadia National Park, Maine, USA. *Water, Air, Soil Pollut.* **2006**, *170* (1−4), 249−265.
(28) Carrasco-Gil, S.; Siebner, H.; LeDuc, D. L.; Webb, S. M.; Millan, R.; Andrews, J. C.; Hernandez, L. E. Mercury Localization and Speciation in Plants Grown Hydroponically or in a Natural Environment. *Environ. Sci. Technol.* **2013**, *47* (7), 3082−3090.
(29) Jiskra, M.; Wiederhold, J. G.; Skyllberg, U.; Kronberg, R. M.; Hajdas, I.; Kretzschmar, R. Mercury Deposition and Re-emission Pathways in Boreal Forest Soils Investigated with Hg Isotope Signatures. *Environ. Sci. Technol.* **2015**, *49* (12), 7188−7196.
(30) Zhou, J.; Feng, X. B.; Liu, H. Y.; Zhang, H.; Fu, X. W.; Bao, Z. D.; Wang, X.; Zhang, Y. P. Examination of total mercury inputs by precipitation and litterfall in a remote upland forest of Southwestern China. *Atmos. Environ.* **2013**, *81*, 364−372.
(31) Wang, J.; Feng, X.; Anderson, C. W. N.; Qiu, G.; Ping, L.; Bao, Z. Ammonium thiosulphate enhanced phytoextraction from mercury contaminated soil-Results from a greenhouse study. *J. Hazard. Mater.* **2011**, *186* (1), 119−127.
(32) Olson, M. L.; DeWild, J. F., Techniques for the collection and species-specific analysis of low levels of mercury in water, sediment, and biota, In: Morganwalp, D. W., Buxton, H. T. Eds.; *U.S. Geological Survey Toxic Substances Hydrology Program, Proceedings of the Technical Meeting. U.S. Geological Survey*, Charleston, SC, pp 191−200, March 8−12, 1999.
(33) Feng, X.; Li, P.; Qiu, G.; Wang, S.; Li, G.; Shang, L.; Meng, B.; Jiang, H.; Bai, W.; Li, Z. Human exposure to methylmercury through rice intake in mercury mining areas, Guizhou Province, China. *Environ. Sci. Technol.* **2008**, *42* (1), 326−332.
(34) Hintelmann, H.; Ogrinc, N. Determination of stable mercury isotopes by ICP/MS and their application in environmental studies. *Acs. Sym. Ser.* **2002**, *835*, 321−338.
(35) Wang, R.; Feng, X. B.; Wang, W. X. In Vivo Mercury Methylation and Demethylation in Freshwater Tilapia Quantified by Mercury Stable Isotopes. *Environ. Sci. Technol.* **2013**, *47* (14), 7949−7957.
(36) Cui, L. W.; Feng, X. B.; Lin, C. J.; Wang, X. M.; Meng, B.; Wang, X.; Wang, H. Accumulation and Translocation of (198)Hg in Four Crop Species. *Environ. Toxicol. Chem.* **2014**, *33* (2), 334−340.
(37) Blum, J. D. Applications of stable mercury isotopes to biogeochemistry. *Handbook of Environmental Isotope Geochemistry* **2012**, 229−245.
(38) Spedding, D. J.; Hamilton, R. B. Adsorption of Mercury-Vapor by Indoor Surfaces. *Environ. Res.* **1982**, *29* (1), 30−41.
(39) Dumarey, R.; Dams, R.; Hoste, J. Comparison of the collection and desorption efficiency of activated charcoal, silver, and gold for the determination of vapor-phase atmospheric mercury. *Anal. Chem.* **1985**, *57* (13), 2638−2643.
(40) Hintelmann, H.; Harris, R.; Heyes, A.; Hurley, J. P.; Kelly, C. A.; Krabbenhoft, D. P.; Lindberg, S.; Rudd, J. W.; Scott, K. J.; St. Louis, V. L. Reactivity and mobility of new and old mercury deposition in a boreal forest ecosystem during the first year of the METAALICUS study. *Environ. Sci. Technol.* **2002**, *36* (23), 5034−5040.
(41) Ericksen, J. A.; Gustin, M. S.; Lindberg, S. E.; Olund, S. D.; Krabbenhoft, D. P. Assessing the potential for re-emission of mercury deposited in precipitation from arid soils using a stable isotope. *Environ. Sci. Technol.* **2005**, *39* (20), 8001−8007.

DOI: 10.1021/acs.est.8b06343
Environ. Sci. Technol. 2019, 53, 4869−4879

(42) McClaugherty, C. A.; Pastor, J.; Aber, J. D.; Melillo, J. M. Forest litter decomposition in relation to soil nitrogen dynamics and litter quality. *Ecology* **1985**, *66*, 266−275.
(43) Hobbie, S. E. Temperature and plant species control over litter decomposition in Alaskan tundra. *Ecol. Monogr.* **1996**, *66* (4), 503−522.
(44) Jianfen, G.; Yusheng, Y.; Guangshui, C.; Peng, L.; Jinsheng, X. A review on litter decomposition in forest ecosystem. *Scientia Silvae Sinicae* **2006**, *42* (4), 93−100.
(45) O'Connell, A. M. Litter decomposition, soil respiration and soil chemical and biochemical properties at three contrasting sites in karri (*Eucalyptus diversicolor* F. Muell.) forests of southwestern Australia. *Australian journal of ecology* **1987**, *12* (1), 31−40.
(46) Swift, M. J., Heal, O. W.; Anderson, J. M. *Decomposition in Terrestrial Ecosystems*;Blackwell Scientific Publications Ltd: Oxford, U.K., 1979.
(47) Hissler, C.; Probst, J. L. Impact of mercury atmospheric deposition on soils and streams in a mountainous catchment (Vosges, France) polluted by chlor-alkali industrial activity: The important trapping role of the organic matter. *Sci. Total Environ.* **2006**, *361* (1), 163−178.
(48) Laurier, F.; Cossa, D.; Gonzalez, J. L.; Breviere, E.; Sarazin, G. Mercury transformations and exchanges in a high turbidity estuary: The role of organic matter and amorphous oxyhydroxides. *Geochim. Cosmochim. Acta* **2003**, *67* (18), 3329−3345.
(49) Kogel-Knabner, I. The macromolecular organic composition of plant and microbial residues as inputs to soil organic matter. *Soil Biol. Biochem.* **2002**, *34* (2), 139−162.
(50) Bugg, T. D. H.; Ahmad, M.; Hardiman, E. M.; Rahmanpour, R. Pathways for degradation of lignin in bacteria and fungi. *Nat. Prod. Rep.* **2011**, *28* (12), 1883−1896.
(51) Longe, L. F.; Couvreur, J.; Grandchamp, M. L.; Garnier, G.; Allais, F.; Saito, K. Importance of Mediators for Lignin Degradation by Fungal Laccase. *ACS Sustainable Chem. Eng.* **2018**, *6* (8), 10097−10107.
(52) Ferreira, V.; Chauvet, E. Future increase in temperature more than decrease in litter quality can affect microbial litter decomposition in streams. *Oecologia* **2011**, *167* (1), 279−291.
(53) Yin, X. W.; Perry, J. A.; Dixon, R. K. Influence of Canopy Removal on Oak Forest Floor Decomposition. *Can. J. For. Res.* **1989**, *19* (2), 204−214.
(54) Whitford, W. G.; Meentemeyer, V.; Seastedt, T. R.; Cromack, K.; Crossley, D. A.; Santos, P.; Todd, R. L.; Waide, J. B. Exceptions to the Aet Model - Deserts and Clear-Cut Forest. *Ecology* **1981**, *62* (1), 275−277.
(55) Ma, M.; Du, H. X.; Wang, D. Y.; Sun, T.; Sun, S. W.; Yang, G. The fate of mercury and its relationship with carbon, nitrogen and bacterial communities during litter decomposing in two subtropical forests. *Appl. Geochem.* **2017**, *86*, 26−35.
(56) Demers, J. D.; Driscoll, C. T.; Fahey, T. J.; Yavitt, J. B. Mercury cycling in litter and soil in different forest types in the Adirondack region, New York, USA. *Ecol. Appl.* **2007**, *17* (5), 1341−1351.
(57) Hall, B. D.; Louis, V. L. S. Methylmercury and total mercury in plant litter decomposing in upland forests and flooded landscapes. *Environ. Sci. Technol.* **2004**, *38* (19), 5010−5021.
(58) Stamenkovic, J.; Gustin, M. S. Nonstomatal versus Stomatal Uptake of Atmospheric Mercury. *Environ. Sci. Technol.* **2009**, *43* (5), 1367−1372.
(59) Obrist, D.; Johnson, D. W.; Lindberg, S. E.; Luo, Y.; Hararuk, O.; Bracho, R.; Battles, J. J.; Dail, D. B.; Edmonds, R. L.; Monson, R. K.; Ollinger, S. V.; Pallardy, S. G.; Pregitzer, K. S.; Todd, D. E. Mercury Distribution Across 14 US Forests. Part I: Spatial Patterns of Concentrations in Biomass, Litter, and Soils. *Environ. Sci. Technol.* **2011**, *45* (9), 3974−3981.
(60) Demers, J. D.; Yavitt, J. B.; Driscoll, C. T.; Montesdeoca, M. R. Legacy mercury and stoichiometry with C, N, and S in soil, pore water, and stream water across the upland-wetland interface: The influence of hydrogeologic setting. *J. Geophys. Res.: Biogeosci.* **2013**, *118* (2), 825−841.
(61) Navratil, T.; Shanley, J.; Rohovec, J.; Hojdova, M.; Penizek, V.; Buchtova, J. Distribution and Pools of Mercury in Czech Forest Soils. *Water, Air, Soil Pollut.* **2014**, *225* (3), 1 DOI: 10.1007/s11270-013-1829-1.
(62) Gruba, P.; Socha, J.; Pietrzykowski, M.; Pasichnyk, D. Tree species affects the concentration of total mercury (Hg) in forest soils: Evidence from a forest soil inventory in Poland. *Sci. Total Environ.* **2019**, *647*, 141−148.
(63) Blackwell, B. D.; Driscoll, C. T. Using foliar and forest floor mercury concentrations to assess spatial patterns of mercury deposition. *Environ. Pollut.* **2015**, *202*, 126−134.
(64) Schwesig, D.; Matzner, E. Dynamics of mercury and methylmercury in forest floor and runoff of a forested watershed in Central Europe. *Biogeochemistry* **2001**, *53* (2), 181−200.
(65) Zhou, J.; Wang, Z. W.; Zhang, X. S. Deposition and Fate of Mercury in Litterfall, Litter, and Soil in Coniferous and Broad-Leaved Forests. *J. Geophys. Res.: Biogeosci.* **2018**, *123* (8), 2590−2603.
(66) Feng, X. B.; Wang, S. F.; Qiu, G. A.; Hou, Y. M.; Tang, S. L. Total gaseous mercury emissions from soil in Guiyang, Guizhou, China. *Journal of Geophysical Research: Atmospheres* **2005**, *110* (D14), 5643 DOI: 10.1029/2004JD005643.
(67) Gustin, M. S.; Rasmussen, P.; Edwards, G.; Schroeder, W.; Kemp, J. Application of a laboratory gas exchange chamber for assessment of in situ mercury emissions. *Journal of Geophysical Research: Atmospheres* **1999**, *104* (D17), 21873−21878.
(68) Xiao, Z. F.; Munthe, J.; Schroeder, W. H.; Lindqvist, O. Vertical Fluxes of Volatile Mercury over Forest Soil and Lake Surfaces in Sweden. *Tellus, Ser. B* **1991**, *43* (3), 267−279.
(69) Ma, M.; Wang, D. Y.; Sun, R. G.; Shen, Y. Y.; Huang, L. X. Gaseous mercury emissions from subtropical forested and open field soils in a national nature reserve, southwest China. *Atmos. Environ.* **2013**, *64*, 116−123.
(70) Gustin, M. S.; Lindberg, S. E. Assessing the contribution of natural sources to the global mercury cycle: The importance of intercomparing dynamic flux measurements. *Fresenius' J. Anal. Chem.* **2000**, *366* (5), 417−422.
(71) Eckley, C. S.; Gustin, M.; Lin, C. J.; Li, X.; Miller, M. B. The influence of dynamic chamber design and operating parameters on calculated surface-to-air mercury fluxes. *Atmos. Environ.* **2010**, *44* (2), 194−203.
(72) Lin, C. J.; Zhu, W.; Li, X. C.; Feng, X. B.; Sommar, J.; Shang, L. H. Novel Dynamic Flux Chamber for Measuring Air-Surface Exchange of Hg-o from Soils. *Environ. Sci. Technol.* **2012**, *46* (16), 8910−8920.
(73) Zhu, W.; Sommar, J.; Lin, C. J.; Feng, X. Mercury vapor air−surface exchange measured by collocated micrometeorological and enclosure methods - Part II: Bias and uncertainty analysis. *Atmos. Chem. Phys.* **2015**, *15* (10), 5359−5376.
(74) Zhu, W.; Sommar, J.; Lin, C. J.; Feng, X. Mercury vapor air−surface exchange measured by collocated micrometeorological and enclosure methods - Part I: Data comparability and method characteristics. *Atmos. Chem. Phys.* **2015**, *15* (2), 685−702.
(75) Fu, X. W.; Feng, X. B.; Sommar, J.; Wang, S. F. A review of studies on atmospheric mercury in China. *Sci. Total Environ.* **2012**, *421*, 73−81.
(76) Zhu, W.; Lin, C. J.; Wang, X.; Sommar, J.; Fu, X. W.; Feng, X. B. Global observations and modeling of atmosphere-surface exchange of elemental mercury: a critical review. *Atmos. Chem. Phys.* **2016**, *16* (7), 4451−4480.
(77) Ma, M.; Wang, D. Y.; Du, H. X.; Sun, T.; Zhao, Z.; Wang, Y. M.; Wei, S. Q. Mercury dynamics and mass balance in a subtropical forest, southwestern China. *Atmos. Chem. Phys.* **2016**, *16* (7), 4529−4537.
(78) Wang, Z. W.; Zhang, X. S.; Xiao, J. S.; Zhijia, C.; Yu, P. Z. Mercury fluxes and pools in three subtropical forested catchments, southwest China. *Environ. Pollut.* **2009**, *157* (3), 801−808.
(79) Zhou, J.; Wang, Z. W.; Sun, T.; Zhang, H.; Zhang, X. S. Mercury in terrestrial forested systems with highly elevated mercury

deposition in southwestern China: The risk to insects and potential release from wildfires. *Environ. Pollut.* **2016**, *212*, 188−196.
(80) Song, S.; Selin, N. E.; Soerensen, A. L.; Angot, H.; Artz, R.; Brooks, S.; Brunke, E. G.; Conley, G.; Dommergue, A.; Ebinghaus, R.; Holsen, T. M.; Jaffe, D. A.; Kang, S.; Kelley, P.; Luke, W. T.; Magand, O.; Marumoto, K.; Pfaffhuber, K. A.; Ren, X.; Sheu, G. R.; Slemr, F.; Warneke, T.; Weigelt, A.; Weiss-Penzias, P.; Wip, D. C.; Zhang, Q. Top-down constraints on atmospheric mercury emissions and implications for global biogeochemical cycling. *Atmos. Chem. Phys.* **2015**, *15* (12), 7103−7125.
(81) Agnan, Y.; Le Dantec, T.; Moore, C. W.; Edwards, G. C.; Obrist, D. New Constraints on Terrestrial Surface Atmosphere Fluxes of Gaseous Elemental Mercury Using a Global Database. *Environ. Sci. Technol.* **2016**, *50* (2), 507−524.
(82) Obrist, D. Mercury Distribution across 14 U.S. Forests. Part II: Patterns of Methyl Mercury Concentrations and Areal Mass of Total and Methyl Mercury. *Environ. Sci. Technol.* **2012**, *46* (11), 5921−5930.
(83) De Lima, C. A. I.; De Almeida, M. G.; Pestana, I. A.; Bastos, W. R.; Recktenvald, M. C. N. D.; De Souza, C. M. M.; Pedrosa, P. Impact of Land Use on the Mobility of Hg Species in Different Compartments of a Tropical Watershed in Brazil. *Arch. Environ. Contam. Toxicol.* **2017**, *73* (4), 578−592.
(84) Zhang, L. M.; Wu, Z. Y.; Cheng, I.; Wright, L. P.; Olson, M. L.; Gay, D. A.; Risch, M. R.; Brooks, S.; Castro, M. S.; Conley, G. D.; Edgerton, E. S.; Holsen, T. M.; Luke, W.; Tordon, R.; Weiss-Penzias, P. The Estimated Six-Year Mercury Dry Deposition Across North America. *Environ. Sci. Technol.* **2016**, *50* (23), 12864−12873.
(85) Risch, M. R.; DeWild, J. F.; Gay, D. A.; Zhang, L. M.; Boyer, E. W.; Krabbenhoft, D. P. Atmospheric mercury deposition to forests in the eastern USA. *Environ. Pollut.* **2017**, *228*, 8−18.
(86) Lu, W. J.; Liu, N.; Zhang, Y. J.; Zhou, J. Q.; Guo, Y. P.; Yang, X. Impact of vegetation community on litter decomposition: Evidence from a reciprocal transplant study with C-13 labeled plant litter. *Soil Biol. Biochem.* **2017**, *112*, 248−257.

DOI: 10.1021/acs.est.8b06343
Environ. Sci. Technol. 2019, 53, 4869−4879